Hindawi Publishing Corporation
International Journal of Photoenergy
Volume 2010, Article ID 268035, 6 pages
doi:10.1155/2010/268035

Research Article

Investigation of Low-Cost Surface Processing Techniques for Large-Size Multicrystalline Silicon Solar Cells

Yuang-Tung Cheng,[1] Jyh-Jier Ho,[1] William J. Lee,[2] Song-Yeu Tsai,[2] Yung-An Lu,[1] Jia-Jhe Liou,[1] Shun-Hsyung Chang,[3] and Kang L. Wang[4]

[1] *Department of Electrical Engineering, National Taiwan Ocean University, No. 2 Pei-ning Rd., Keelung 20224, Taiwan*
[2] *Photovoltaics Technology Center, Industrial Technology Research Institute, No. 195 Chung Hsing Rd., 4 Sec. Chu Tung, Hsin Chu 31061, Taiwan*
[3] *Department of Microelectronic Engineering, National Kaohsiung Marine University, No. 142 Haijhuan Rd., Kaohsiung 81143, Taiwan*
[4] *Device Research Laboratory, Department of Electrical Engineering, University of California, Los Angeles, CA 90095, USA*

Correspondence should be addressed to Jyh-Jier Ho, jackho@mail.ntou.edu.tw

Received 2 January 2010; Revised 8 March 2010; Accepted 13 March 2010

Academic Editor: Mario Pagliaro

The subject of the present work is to develop a simple and effective method of enhancing conversion efficiency in large-size solar cells using multicrystalline silicon (mc-Si) wafer. In this work, industrial-type mc-Si solar cells with area of 125×125 mm^2 were acid etched to produce simultaneously $POCl_3$ emitters and silicon nitride deposition by plasma-enhanced chemical vapor deposited (PECVD). The study of surface morphology and reflectivity of different mc-Si etched surfaces has also been discussed in this research. Using our optimal acid etching solution ratio, we are able to fabricate mc-Si solar cells of 16.34% conversion efficiency with double layers silicon nitride (Si_3N_4) coating. From our experiment, we find that depositing double layers silicon nitride coating on mc-Si solar cells can get the optimal performance parameters. Open circuit (V_{oc}) is 616 mV, short circuit current (J_{sc}) is 34.1 mA/cm^2, and minority carrier diffusion length is 474.16 μm. The isotropic texturing and silicon nitride layers coating approach contribute to lowering cost and achieving high efficiency in mass production.

1. Introduction

The multicrystalline silicon (mc-Si) solar cell is not only still heavily dependent on the material base in the semiconductor industry, but also features an excellent stability, mature technology, and easy acquisition [1, 2]. It also satisfies these requirements for the rapidly expanding solar energy markets [3–6]. The main reason why mc-Si solar cells are widely used is that mc-Si solar cells own the highest growth rate and the lowest fabrication cost in the mass-production level [5, 6]. Even though some commercial Si solar cell panels from company such as Samsung have above 18% conversion efficiency on float zone (FZ) Si wafers [7, 8], the structure of passivated emitter and rear cell is more complicated by using several expensive photolithography processes. However, the production of crystalline silicon (c-Si) solar cell with such a high efficiency is very small compared to that of conventional Si solar cell because of complicated fabrication process with cost-intensive process steps and because of their small areas. In order to commercialize high-efficiency solar cell for optional consumer electronics, it is essential to produce cells with low cost on Czochralski (CZ) mc-Si wafers and simple fabrication processes proposed in our research.

The efficiency of mc-Si solar cells is mainly limited by minority carrier recombination. Major mc-Si disadvantages are wide varieties of defects inhomogeneously distributed, such as dislocations, grain boundaries, oxygen clusters, metal impurities, and dangling bond. In any *pn*-junction of the solar-cell process, meanwhile, the emitting electrons inside the c-Si are highly active and easily combine with other elements [9–12]. Besides, the mc-Si defects can lower the efficiency and decrease diffusion length [13–15].

The essential factors of achieving high efficiencies of Si-based wafer are the large minority carrier recombination lifetime and long diffusion length in mc-Si solar cells [16, 17]. Therefore, removing grain boundary on mc-Si surface by texturing is the present key issue of mc-Si research. We use large size CZ mc-Si wafer in order to investigate the influence of the grain boundary on the minority charge carrier diffusion length. Texturing the front surface of a solar cell generally results in performance improvement, because it removes surface damage or roughness and increases in the short-circuit current [18–20]. While the result of the bare wafers indicates a good effectiveness in acid etching experiment, a silicon nitride (Si_3N_4) coated on the surface of a real cell by plasma-enhanced chemical vapor deposited (PECVD) further changes the overall reflection properties. The hydrogen-rich PECVD Si_3N_4 layer can achieve good passivation [21–24]. In this research, a single layer (SL) Si_3N_4 and dual layers (DL) Si_3N_4 are deposited on large size ($125 \times 125\,mm^2$) mc-Si wafers by PECVD. From the experiment, we find that the effect on DL is better than that on SL. Therefore, our experiment mainly focuses on the concept of utilizing the DL refractive index of Si_3N_4 to minimize the reflection losses and passivation of the solar-cell surface.

2. Experiments

A series of experiments on mc-Si texturization were carried out with different approaches. For mc-Si solar cells fabrication, CZ (100)-oriented, p-type, 4-inch diameter, resistivity 1 Ω-cm, size $125 \times 125\,mm^2$, 300-μm thick wafers were used as a base material. The wafers were textured using acidic mixtures containing hydrofluoric acid (HF) and nitric acid (HNO_3) diluted with H_2O. The mixture of HF and HNO_3 was applied in a dipping bath for the removal of contaminations and lattice defects generated by the lapping of Si wafers. The removal of saw damage and the surface texturing are obtained in one step. High etching rate ($\sim 5\,\mu$m/min) is preferable for large-scale production in which many wafers should be texturized in a short time. We have observed from scanning electron microscopy (SEM) micrographs that the Si surface that was etched with acidic solution of HF, HNO_3 and deionized (DI) water in the volume ratio 15 : 1 : 2.5 for 60 seconds showed uniform hemispherical etch pits. This was followed by a clean in 1 : 1 : 5 HCl : H_2O_2 : H_2O for 20 minutes and rinse in DI water. Next the n-type emitter was diffused by phosphorus (P) in open-tube furnace using conventional $POCl_3$ diffusion source at 835°C for 10 minutes predeposition followed by 20 minutes drive-in process.

After phosphorus glass removal and another clean, Si_3N_4 films were deposited by the PECVD in a conventional direct plasma reactor operating at 13.56 MHz using a mixture of the silane (SiH_4) and ammonia (NH_3) and the deposition temperature was set at 450°C. The refractive index (n) of solar cells depends on SiH_4 and NH_3 gas ratio. Common anti-reflection (AR) layer materials are SiO_2 ($n = 1.5$), Si_3N_4 ($n = 2.0$), and TiO_2 ($n = 2.5$) [25, 26]. Figure 1 shows refractive indices of the Si_3N_4 films deposited on the mc-Si wafers at different ratios of gas flow rate and refractive indices during PECVD process. When the ratios of gas flow increase from 3 to 90, the values of n are decreased dramatically initially, then moderately, and n saturated at 1.91 as gas-flow ratio is larger than 75. The optimal n value with thickness (d) allows us to measure the properties of different AR coatings by using elliptical polarizer. Corresponding expressions for the transmission and reflection coefficients are determined. The inset table also shows the measured n with corresponding d values for SL and DL AR films. Therefore, for the SL coating, the measured values for n_1 and d_1 are 2.05 and 86 nm, respectively. For DL coating, the measured upper layer parameters of n_1 and d_1 are 1.91 and 66 nm and the measured bottom layer parameters of n_2 and d_2 are 2.05 and 36 nm, respectively.

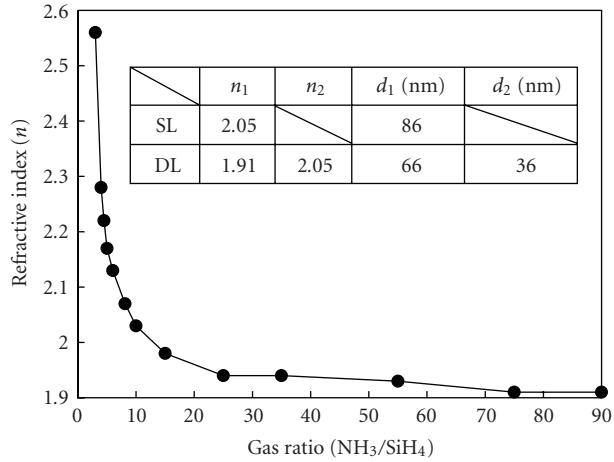

	n_1	n_2	d_1 (nm)	d_2 (nm)
SL	2.05		86	
DL	1.91	2.05	66	36

Figure 1: Refractive indices (n) of Si_3N_4 films deposited with different ratios of gas-flow rate. The inset table is the measured n with corresponding thickness (d) values for SL and DL AR films.

The front and back metallizations of the diffused mc-Si wafers were carried out using standard Ag-paste and Al paste for screen-printed metallization technique followed by baking and cofiring at a temperature of 750°C in a conveyer belt furnace. Finally, the solar cells were edge isolated using a dicing saw. For simplification of terrestrial solar-cell characterization, the induced current density-voltage (J-V) curves of the developed devices were measured under the air mass (AM1.5G) of the solar simulator (Wacom, Model: WXS-220S-L2) illumination at $1000\,W/m^2$ on a Keithley 4200 instrument. The quality of the surface passivation was revealed by lifetime measurements, which were obtained by Semilab WT-2000. We also measured the sample's quantum efficiency (QE) by PV Measurement (Model: QEX7).

3. Treatment Result and Discussion

A series of experiments on mc-Si texturization were carried out with different approaches. Our first results regarding the variation of the morphological studies of different hemispherical structure are formed in large area $125 \times 125\,mm^2$ mc-Si wafer. For the theoretical approach to get

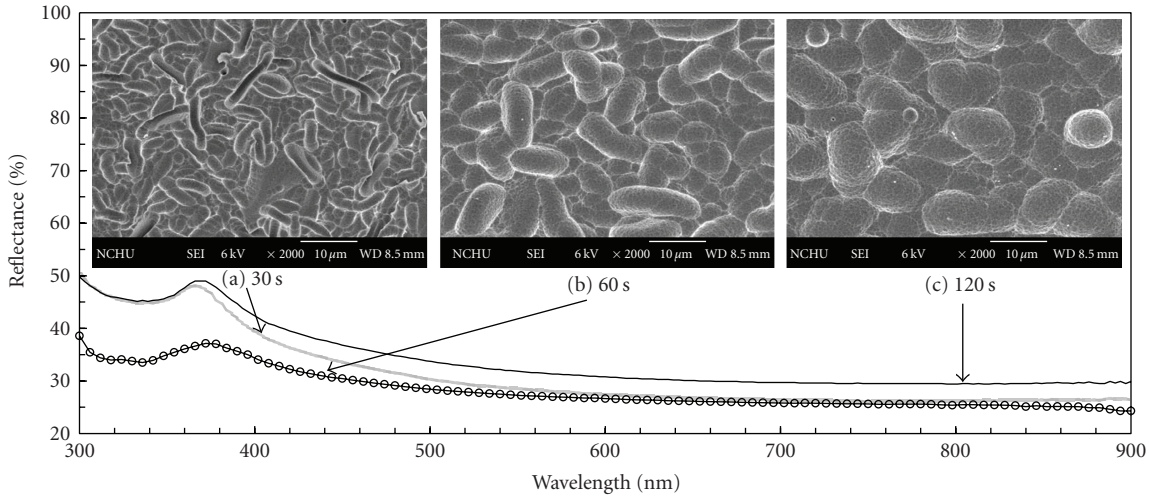

FIGURE 2: Reflectivity of the textured mc-Si surfaces after 30 seconds, 60 seconds, and 120 seconds of etching in HF : HNO_3 : H_2O = 15 : 2.5 : 1 solution. SEM micrographs of the textured mc-Si surfaces after 30 seconds, 60 seconds, and 120 seconds of etching are shown in inset figure (a), (b), and (c).

lower reflectance, we assumed it to be a part of a sphere for simplicity. The calculation was based on a ray-tracing method. As the texture is a part of a sphere, the relationship between width (D), depth (H), radius (r), and the surface reflectance (R) corresponding with function of incident angle ($f(\theta)$) can be calculated as follows [27]:

$$D^2 = 8rH - 4H^2,$$
$$R \propto \frac{\sum_{i=1}^{n}\left\{[f(\theta)]^i \times \pi r^2\right\}}{\pi(2rH - H^2)}. \quad (1)$$

In other words, the ratio (H/D) of depth and width of these etch pits determines the reflectance of the textured mc-Si [28]. Figures 2(a), 2(b), and 2(c) show the surface morphology after 30, 60, and 120 seconds of acid etching. Acid etching forms spherical etch pits on the surface of mc-Si which are generated by saw damage as template. The resulting surface structure after 30 seconds etching features the known homogeneous arranged oval etch warm shape pits with a mean width of 5–8 μm (shown as Figure 2(a)) and a depth of 2.5 μm. After 60 seconds, the shape changes from oval pits to mainly round structure with an average diameter of 10–15 μm as shown in Figure 2(b). These rounded features have good antireflection properties. After 120 seconds of etching, the shape changes from oval pits to become plainer due to longer etch times or higher etch rates. According to article [27], these structures increase the reflectance of silicon. After thorough observation with an optical microscope, it was found that the surface structures were not yet satisfactory in the case of texturing with three different ratios of HF : HNO_3 : H_2O for etching times over 60 seconds. If the time of etching is too long, the texturization disappears and the dislocations and grains boundary figures appear. The surface of mc-Si is not quite satisfactory for solar cell application even up to 60 seconds of etching as shown in Figure 2(c). Therefore, in the case of mc-Si after 60 etching for the rounds geometry, the lowest reflectance corresponding to a geometry having the highest ratio of H/D was observed. And so it can be concluded that the most reduction of the reflectance is obtained at the optimized etching time of 60 seconds.

The reflectance is minimal for high ratios of H/D. Since the surface structure and precisely the ratio H/D are highly sensitive to the slightest changes in the reaction of the etchant, all influencing parameters arising during the electrochemical process like etching time and rate should be examined. Figure 2 shows the reflectance of the textured surface for wavelengths between 300 and 900 nm. These curves reveal the increasing importance of the geometry comparing to the etch time. Compared with that of the textured surface, the average reflectance of the mc-Si surface decreased to 25.3% after the acid texturing process while after texturing for 60 seconds, the decrease of the reflectance was rather weak, especially at long wavelengths.A significant reduction of the reflectance which is the optimized etching time for 60 seconds has to be noted.

The samples being acid texturized during 60 seconds were used in the next processes for phosphorus diffusion. The n-type emitter was formed by heavily doping with phosphorus using a $POCl_3$ source at high temperature. Figure 3 illustrates the (1) sheet resistance (in $\Omega/\square$) and (2) conversion efficiency (in %) as a function of different temperatures (from 770°C to 900°C of the solar-cell with drive-in diffusion processes). Among the diffusion process included in the study, the maximum conversion efficiency value of 14.26% is obtained at 835°C diffusion temperature. Further increases in the diffusion temperature beyond 835°C cause decreased conversion efficiency. The sheet resistance decreases initially with increasing the diffusion temperatures, and reaches a minimum value at 835°C -diffusion temperature. With this optimal diffusion parameters at 835°C for a solar-cell prototype, the sheet resistance is measured to be 44.7 $\Omega/\square$, and its corresponding conversion efficiency is 14.26%.

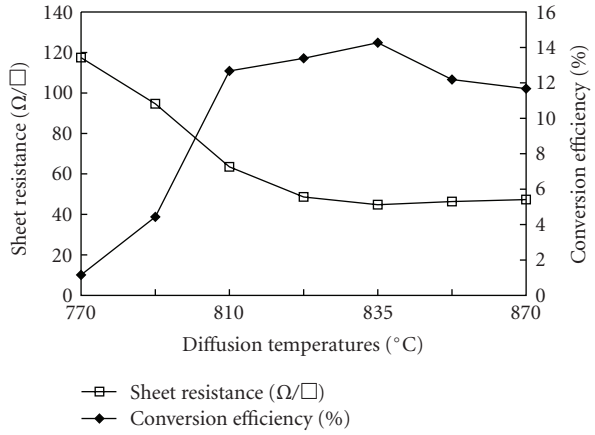

Figure 3: The sheet resistance (in Ω/□) and conversion efficiency (in %) with respect to different temperatures (from 770°C to 900°C) of the solar-cell prototypes with and without drive-in diffusion processes.

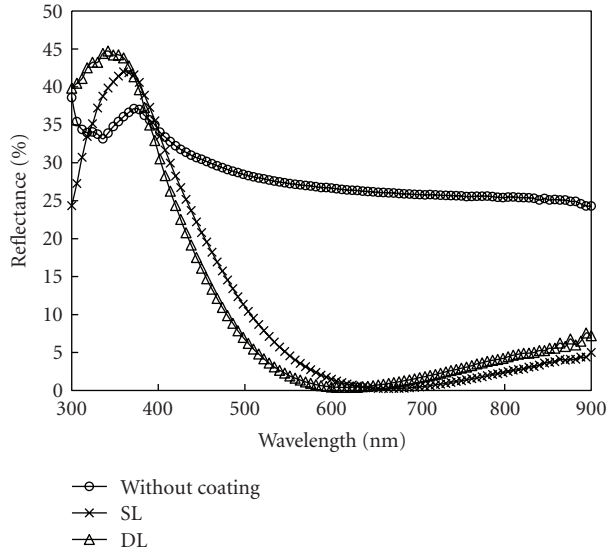

Figure 4: Comparison of reflectance of acid solution textured mc-Si surfaces with (SL, DL) and without Si_3N_4 coating. One can clearly show that the reflectance for the DL coating is a very low value of 1% between 572 nm and 672 nm wavelength.

The surface reflectance was further lowered after depositing Si_3N_4 layer on the large-area surface of the mc-Si solar cell, and the results are shown in Figure 4. The reflectance for the SL coating remains at a low value below 2.8% for an extended spectral range from 612 nm to 738 nm wavelength. In contrast, the reflectance for the DL coating is a very low value of 1% between 572 nm and 672 nm wavelength. We focus our attention on the 450–600 nm spectral range which corresponds to the maximum intensity of solar irradiation. Compared with the SL, the DL coating is characterized by a smaller reflectance precisely in this useful range. The character could significantly contribute to further improvements on solar cells' performance.

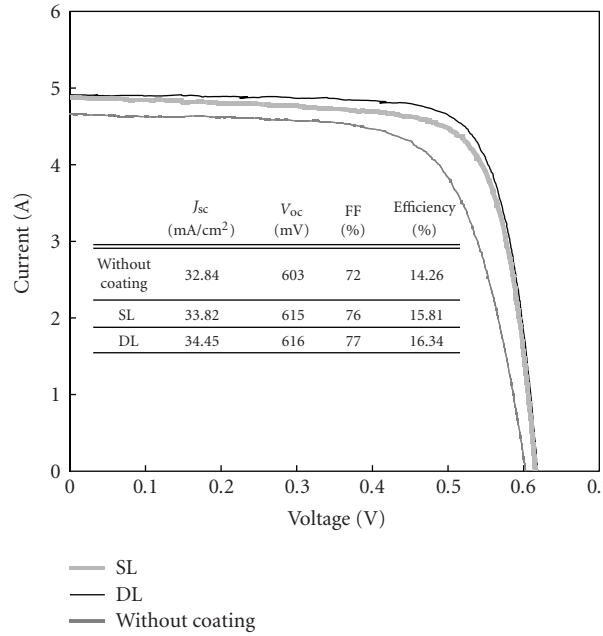

	J_{sc} (mA/cm^2)	V_{oc} (mV)	FF (%)	Efficiency (%)
Without coating	32.84	603	72	14.26
SL	33.82	615	76	15.81
DL	34.45	616	77	16.34

Figure 5: Comparison of IV-curves of a 125 × 125 mm^2 of the different results from DL, SL, and without coating. DL's conversion efficiency is the highest.

As a matter of course, an increase in the light absorbed in the cell properly enhances the generation of electrical parameters of the cell if there is no loss from the deposition scheme. This could be confirmed by measuring of the I-V curve of the developed cell as in Figure 5. The solar cell surface with DL coating and the short-circuit current density (J_{sc}) of 34.45 mA/cm^2 cell are comparable to a solar cell without coating. The observed conversion efficiency (η) was 16.34%, which is a major advantage of Si_3N_4 films. The high conversion efficiency also electronically passivates the surface, leading to reduced recombination losses. To increase DL coating in the lightest absorbed in the cell properly enhances the generation of electron-hole pairs and the current density of the cell if there is no loss from the passivation process. The solar cell with the SL coating had the high efficiency. J_{sc} is 33.82 mA/cm^2, open-circuit voltage (V_{oc}) is 615 mV, fill factor (FF) is 76%, and η is 15.81%. The difference in conversion efficiencies of cells with different surfaces basically comes from the variation of J_{sc}. They are mainly depositing condition-dependent parameter of the large-size solar cells. It seems that the V_{oc} and the FF are clearly not related to the AR coating. With these results, it can be concluded that our deposition scheme with DL coating creating AR surface is successful in achieving better J_{sc} and hence better conversion efficiency in large-area mc-Si solar cell.

The percentage refers to the fraction of light-generated carrier and the variations between one region and another are due to variations in the diffusion length in the solar cell caused by the light absorb in the mc-Si solar cells. Figure 6 shows average diffusion length of the SL and DL anti-reflection deposition in a large size mc-Si solar

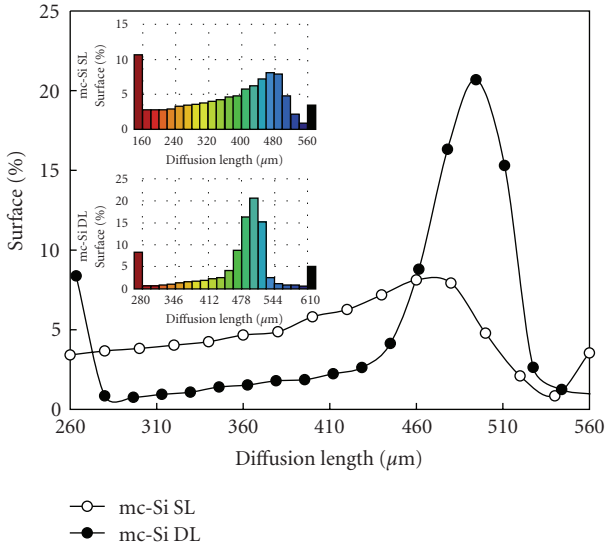

Figure 6: Comparison average diffusion length of the SL and DL antireflection deposition in large size mc-Si solar cell. Histograms of diffusion length against percentage wafer area for SL and DL coating solar cells are shown in the up-left inset.

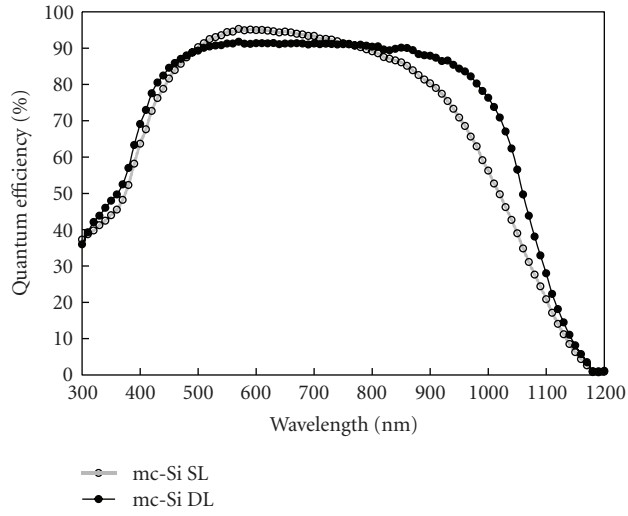

Figure 7: Results of quantum efficiency (QE) measurements SL and DL coated on large size mc-Si solar cells. It clearly shows the DL coating with higher QE in a wavelength range of 450–1000 nm contributed to the lower reflection and the increase in effective minority carrier diffusion length.

cell. Histograms of diffusion length against percentage of large area for SL and DL coating solar cells are shown in the up-left inset. The measured average minority carrier diffusionlengths of SL and DL are 364.97 μm, 474.16 μm, respectively. By comparing the insert histograms for the solar cells deposited with larger size and SL, it can be found that if the cell does not haveenough of the additional hydrogenation through Si_3N_4 passivation, grain boundariesresult in recombination activity. Thus diffusion length is lower. The result obtained using the suggested that graded DL coating is therefore very satisfied, especially if we know that ideal coating layer that we could obtain by complete surface passivation can reduce recombination. Minority carrier lifetimes strongly depend on the passivation process and we found a conversion efficiency of 15.81% and 16.34% for SL and DL, respectively.

Figure 7 shows that the QE curve of the DL coated solar cell is higher than that of the SL coated solar cell in a wide-wavelength range (300–1200 nm). The DL coating having higher QE in a wavelength range of 450–1000 nm contributed to the lower reflection and the increase in effective minority carrier diffusion length. It is also seen that the SL QE decreases in the long wavelength region due to decrease in effective minority carrier diffusion length. This indicates a clear coat quality improvement and since the area under the curve is a measure for the cell current, one can see that the cell with the passivating Si_3N_4 has a higher short circuit current density and thus higher conversion efficiency.

4. Conclusion

For the large size solar cell process described above, an efficiency of 16.34% is achieved. We have shown that the major advantages of the process are texture of a large size mc-Si with suitable acid solution ratio, no grain-boundary delineation, and significant reproducibility. These advantages improve the throughput in industrial production of solar cells. The n-type emitter was formed in the solar cell process by phosphorus diffusion at temperatures of 835°C for 10 minutes predeposition followed by 20 minutes drive-in. By the PECVD, Si_3N_4 layers provide both surface passivation and antireflection coating in silicon solar cells. In this work, the Si_3N_4 films with different refractive indices were prepared by varying the gas flow rate ratio of SiH_4 to NH_3. The DL coated refractive index Si_3N_4 concept demonstrated that this could be used to decrease the reflection losses and surface hydrogen passivation. The increase in J_{sc} is an improvement in the number of layer coating and material thickness, especially for the minority carrier lifetime. The quantum efficiency measurements showed that the DL improvement in average diffusion length has been achieved compared to SL. Because the chemical etching for acid texturization and AR coating formation is very simple, cheap, and suitable for mass production, present technology is very promising for large-area mc-Si solar cells manufacturing. In the future, we will focus both on improving the mc-Si texturing quality and on implementing novel process features like different materials coating to obtain relatively high efficiency solar cells.

Acknowledgment

The authors acknowledge the financial support from *The National Science Council of R.O.C.* under contracts No. NSC 98-2622-E-019-006-CC3 and NSC 98-2221-E-019-003.

References

[1] A. Jäger-Waldau, *PV Status Report 2008*, European Commission, DG Joint Research Centre, Ispra, Italy, 2008.

[2] G. P. Willeke, "Thin crystalline silicon solar cells," *Solar Energy Materials & Solar Cells*, vol. 72, no. 1–4, pp. 191–200, 2002.

[3] L. Sherwood, "U.S. solar market trends 2008," Annual Report, pp. 1–16, Interstate Renewable Energy Council, 2009.

[4] Photovoltaic Technology Research Advisory Council (PV-TRAC) of European Commission, "A vision for photovoltaic technology," Tech. Rep., European Communities, Luxembourg, Belgium, 2005.

[5] A. Goetzberger, C. Hebling, and H.-W. Schock, "Photovoltaic materials, history, status and outlook," *Materials Science and Engineering R*, vol. 40, no. 1, pp. 1–46, 2003.

[6] A. Goetzberger, J. Luther, and G. Willeke, "Solar cells: past, present, future," *Solar Energy Materials and Solar Cells*, vol. 74, no. 1–4, pp. 1–11, 2002.

[7] I. S. Moon, D. S. Kim, and S. H. Lee, "New method for patterning the rear passivation layers of high-efficiency solar cells," *Journal of Materials Science*, vol. 12, no. 10, pp. 605–607, 2001.

[8] J. Kim, J. Hong, and S. H. Lee, "Application of PECVD SiNx films to screen-printed multicrystalline silicon solar cell," *Journal of the Korean Physical Society*, vol. 44, no. 2, pp. 479–482, 2004.

[9] P. Kittidachachan, T. Markvart, D. M. Bagnall, R. Greef, and G. J. Ensell, "A detailed study of p-n junction solar cells by means of collection efficiency," *Solar Energy Materials & Solar Cells*, vol. 91, no. 2-3, pp. 160–166, 2007.

[10] A. G. Aberle, B. Kuhlmann, R. Meyer, A. Hübner, C. Hampe, and R. Hezel, "Comparison of p-n junction and inversion-layer silicon solar cells by means of experiment and simulation," *Progress in Photovoltaics: Research and Applications*, vol. 4, no. 3, pp. 193–204, 1996.

[11] N. M. Johnson and C. Herring, "Hydrogen immobilization in silicon p-n junctions," *Physical Review B*, vol. 38, no. 2, pp. 1581–1584, 1988.

[12] A. G. Aberle, "Surface passivation of crystalline silicon solar cells: a review," *Progress in Photovoltaics: Research and Applications*, vol. 8, no. 5, pp. 473–487, 2000.

[13] B. Sopori, M. I. Symko, R. Reedy, K. Jones, and R. Matson, "Mechanism(s) of hydrogen diffusion in silicon solar cells during forming gas anneal," in *Proceedings of the 26th IEEE Photovoltaic Specialists Conference (PVSC '97)*, pp. 25–30, Anaheim, Calif, USA, September-October 1997.

[14] B. L. Sopori, X. Deng, J. P. Benner, et al., "Hydrogen in silicon: a discussion of diffusion and passivation mechanisms," *Solar Energy Materials and Solar Cells*, vol. 41-42, pp. 159–169, 1996.

[15] P. Sana, A. Rohatgi, J. P. Kalejs, and R. O. Bell, "Gettering and hydrogen passivation of edge-defined film-fed grown multicrystalline silicon solar cells by Al diffusion and forming gas anneal," *Applied Physics Letters*, vol. 64, no. 1, pp. 97–99, 1994.

[16] P. Würfel, T. Trupke, T. Puzzer, E. Schäffer, W. Warta, and S. W. Glunz, "Diffusion lengths of silicon solar cells from luminescence images," *Journal of Applied Physics*, vol. 101, no. 12, Article ID 123110, 10 pages, 2007.

[17] P. S. Plekhanov, R. Gafiteanu, U. M. Gösele, and T. Y. Tan, "Modeling of gettering of precipitated impurities from Si for carrier lifetime improvement in solar cell applications," *Journal of Applied Physics*, vol. 86, no. 5, pp. 2453–2458, 1999.

[18] M. Steinert, J. Acker, A. Henßge, and K. Wetzig, "Experimental studies on the mechanism of wet chemical etching of silicon in HF/HNO_3 mixtures," *Journal of the Electrochemical Society*, vol. 152, no. 12, pp. C843–C850, 2005.

[19] M. Lipiński, P. Panek, and R. Ciach, "The industrial technology of crystalline silicon solar cells," *Journal of Optoelectronics and Advanced Materials*, vol. 5, no. 5, pp. 1365–1371, 2003.

[20] M. S. Kulkarni and H. F. Erk, "Acid-based etching of silicon wafers: mass-transfer and kinetic effects," *Journal of the Electrochemical Society*, vol. 147, no. 1, pp. 176–188, 2000.

[21] L. Carnel, H. Dekkers, I. Gordon, et al., "Study of the hydrogenation mechanism by rapid thermal anneal of siN:H in thin-film polycrystalline-silicon solar cells," *IEEE Electron Device Letters*, vol. 27, no. 3, pp. 163–165, 2006.

[22] J.-J. Ho, C.-Y. Chen, R. Y. Hsiao, and O. L. Ho, "The work function improvement on indium-tin-oxide epitaxial layers by doping treatment for organic light-emitting device applications," *Journal of Physical Chemistry C*, vol. 111, no. 23, pp. 8372–8376, 2007.

[23] J.-J. Ho, C.-Y. Chen, C.-M. Huang, W. J. Lee, W.-R. Liou, and C.-C. Chang, "Ion-assisted sputtering deposition of antireflection film coating for flexible liquid-crystal display applications," *Applied Optics*, vol. 44, no. 29, pp. 6176–6180, 2005.

[24] J.-J. Ho and C.-Y. Chen, "Power effects in indium-zinc oxide thin films for OLEDs on flexible applications," *Journal of the Electrochemical Society*, vol. 152, no. 1, pp. G57–G61, 2005.

[25] F. J. Beck, A. Polman, and K. R. Catchpole, "Tunable light trapping for solar cells using localized surface plasmons," *Journal of Applied Physics*, vol. 105, no. 11, Article ID 114310, 7 pages, 2009.

[26] A. Lennie, H. Abdullah, S. M. Mustaza, and K. Sopian, "Photovoltaic properties of Si_3N_4 layer on silicon solar cell using Silvaco software," *European Journal of Scientific Research*, vol. 29, no. 4, pp. 447–453, 2009.

[27] Y. Nishimoto, T. Ishihara, and K. Namba, "Investigation of acidic texturization for multicrystalline silicon solar cells," *Journal of the Electrochemical Society*, vol. 146, no. 2, pp. 457–461, 1999.

[28] Z. Xi, D. Yang, W. Dan, C. Jun, X. Li, and D. Que, "Texturization of cast multicrystalline silicon for solar cells," *Semiconductor Science and Technology*, vol. 19, no. 3, pp. 485–489, 2004.